Journal of Medicinal Chemistry

Brief Article

pubs.acs.org/jmc

Short Hydrophobic Peptides with Cyclic Constraints Are Potent Glucagon-like Peptide-1 Receptor (GLP-1R) Agonists

Huy N. Hoang,[†] Kun Song,[‡] Timothy A. Hill,[†] David R. Derksen,[∥] David J. Edmonds,[‡] W. Mei Kok,[†] Chris Limberakis,[§] Spiros Liras,[‡] Paula M. Loria,[∥] Vincent Mascitti,[§] Alan M. Mathiowetz,[‡] Justin M. Mitchell,[†] David W. Piotrowski,[§] David A. Price,[‡] Robert V. Stanton,[‡] Jacky Y. Suen,[†] Jane M. Withka,[§] David A. Griffith,*[,‡] and David P. Fairlie*[,†]

[†]Division of Chemistry and Structural Biology, Institute for Molecular Bioscience, University of Queensland, Brisbane, Queensland 4072, Australia

[‡]Worldwide Medicinal Chemistry, Pfizer Worldwide Research and Development, Cambridge, Massachusetts 02139, United States

[§]Worldwide Medicinal Chemistry, and [∥]Pharmacokinetics, Dynamics and Metabolism, Pfizer Worldwide Research and Development, Groton, Connecticut 06340, United States

Supporting Information

ABSTRACT: Cyclic constraints are incorporated into an 11-residue analogue of the N-terminus of glucagon-like peptide-1 (GLP-1) to investigate effects of structure on agonist activity. Cyclization through linking side chains of residues 2 and 5 or 5 and 9 produced agonists at nM concentrations in a cAMP assay. 2D NMR and CD spectra revealed an N-terminal β-turn and a C-terminal helix that differentially influenced affinity and agonist potency. These structures can inform development of small molecule agonists of the GLP-1 receptor to treat type 2 diabetes.

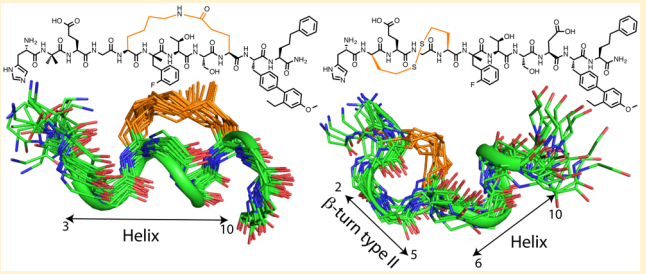

Type 2 diabetes (T2D) is one of the greatest impending global health burdens that already affects >350 million people but is projected to increase to ~600 million by 2035.[1] Glucagon-like peptide-1 (GLP-1) is a naturally occurring hormone that potentiates glucose-dependent insulin secretion from the pancreas, while stimulating proliferation and inhibiting apoptosis of pancreatic β-cells.[2] It also inhibits food intake and gastric emptying leading to weight loss.[3] Current treatments for T2D include injectable peptide analogues of full-length GLP-1(7−36)-NH_2 (*HAEGTFTSDVSS*-**YLEGQAAKEFIA-WLVKGR**-NH_2),[4] and oral inhibitors of dipeptidyl peptidase IV that protect GLP-1 from cleavage of two residues from its N-terminus.[5] Small molecule oral GLP-1 agonists remain elusive.[6]

The interaction of GLP-1 with its receptor can be partially rationalized as follows. The GLP-1 receptor (GLP-1R) is a G-protein-coupled receptor found on pancreatic islets and other cells that captures the helical C-terminal half (bolded above) of GLP-1 and presents the N-terminal half (italicized above) in an unknown manner to activating residues in the receptor.[7] The recently solved crystal structure of the closely related glucagon receptor was used in conjunction with previously reported mutation studies to propose a binding model for glucagon which shows the first five residues in a flexible conformation binding in a deep binding pocket within the seven-transmembrane region of the structure, while residues from S8 onward are in an α-helical conformation.[8] The proposed binding model also suggests a turn type motif between residues 4 and 7.[8] Removing the two N-terminal residues (His-Ala) or more than 3 C-terminal residues of GLP-1(7−36)-NH_2 attenuated activity.[9]

The most successful downsizing of GLP-1 is a series of 11 amino acid peptides (Scheme 1) bearing bulky hydrophobic substituents (X) at positions 6, 10, and 11 which potently activate GLP-1R.[10,11]

Here we report biophysical (NMR) and computational guided design studies to produce novel cyclized variants of 11-mer peptide **1b** which in turn may inform the design of small, orally

Scheme 1. Eleven Residue Peptides (1a, 1b) That Activate GLP-1R

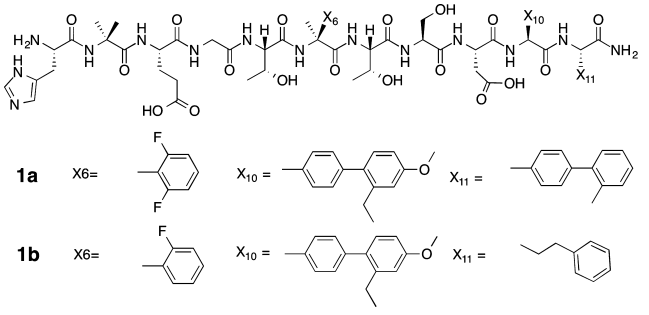

Received: January 29, 2015

DOI: 10.1021/acs.jmedchem.5b00166
J. Med. Chem. XXXX, XXX, XXX−XXX

available GLP-1R agonists. The NMR-derived helical structure of **1a** was determined under conditions (25 mM SDS-d_{25} in H_2O) that simulate to some extent a water-membrane environment (Figure 1A) that may be relevant for the binding of **1a** to the membrane-spanning GLP-1R. VT-NMR data ($\Delta\delta/T \leq 4$ ppb/K) and NOE correlations ($d_{\alpha N(i,i+3)}$, $d_{\alpha N(i,i+4)}$) supported some helical structure between residues 4−11 (Figure 2A). N-terminal residues 1−3 were disordered, but stronger $d_{\alpha N(i,i+2}$ than $d_{\alpha N(i,i+4)}$ NOEs in this region suggested a turn conformation. The Cα···Cα distance (6.1 Å) between residue 5 and residue 9 was typical of an α-helix (idealized α-helix, 6.1 Å; idealized 3_{10}-helix, 8.3 Å). A reported NMR structure for **1a** in aqueous dimethyl sulfoxide (1:3 H_2O/DMSO-d_6) suggested instead that residues 6−11 may adopt an elongated (3_{10}) helix.[10] We therefore also determined an NMR structure for **1a** in 1:3 H_2O/DMSO-d_6 (Figure 1B). Under these conditions we found a very slightly elongated α-helix between C-terminal residues 6 and 11, with the average Cα···Cα distance between residues 6 and 10 being 6.3 Å, while the Thr5 Cα···Cα Aib2 separation was 5.6 Å, consistent with a β-turn structure at the N-terminus. These findings prompted us to insert cyclization constraints into the sequence to stabilize an α-helix between residues 6 and 11 or a β-turn at residues 2−5 and to investigate the possible influences of these structural motifs on agonist activity mediated by human GLP-1R.

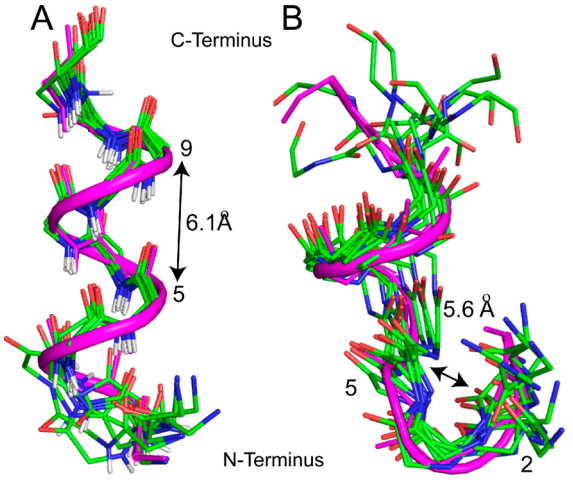

Figure 1. Backbone superimposition of 10 lowest energy refined NMR structures of **1a** in (A) 25 mM SDS-d_{25} in water and (B) H_2O/DMSO-d_6 (1:3). Magenta ribbons show average peptide backbone structures. Arrows show average Cα−Cα distances between residues 5 and 9 (6.1 Å) and residues 2 and 5 (5.6 Å).

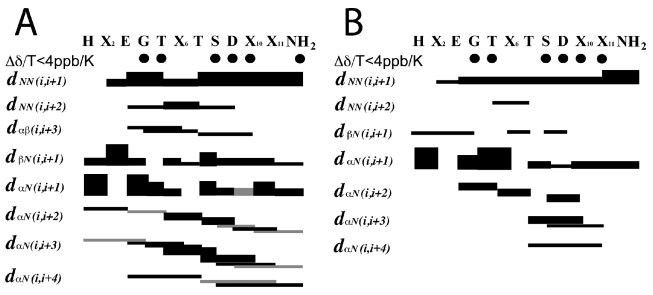

Figure 2. ^{1}H NMR NOE summary for **1a** (1 mM): (A) in 25 mM SDS-d_{25} in H_2O/D_2O (9:1) and (B) in H_2O/DMSO-d_6 (1:3). For sequential and medium range NOEs, bar thickness corresponds to strong (<2.7 Å), medium (<3.5 Å), weak (<5.0 Å), or very weak (<6.0 Å) NOE intensities. Shown are overlapping crosspeaks (gray bars) and amide NH temperature coefficients ($\Delta\delta/T$) of ≤4 ppb/K (●).

Connecting the side chains of residues 5 and 9 in compound **1b** produced analogues **2**−**6**, each with a cyclic constraint of variable ring size at the C-terminus (Table 1). In a cyclic pentapeptide, the linker corresponding to that in **2** is known[12] to enforce more α-helicity than any lactams used in **3**−**6**. Constraining the 11mer peptide with any of these lactam-bridged linkers reduced binding affinity and cAMP activity relative to **1a** and **1b**. However, **2** (EC_{50} = 68 nM) and **3** (EC_{50} = 10 nM) retained appreciable agonist potency. The Lys5→Glu9 lactam bridge in **3** typically[11] promotes a more loosely constrained helix. Expanding the cycle by an additional methylene group through substituting homoglutamate for Glu9 (**4**) further loosened the constraint but substantially reduced agonist potency. Swapping the lactam forming residues in the two most potent compounds (**2** and **3**) substantially reduced cAMP activity (**5** and **6**, respectively), supporting the importance of the location of the lactam and/or helical structure in this segment. Alanine mutagenesis studies have shown that the ninth residue (Asp15) in GLP-1 is crucial for cAMP activity, with complete loss of activity and 40-fold reduction in binding affinity after Asp15Ala substitution.[13] On the other hand the fifth residue (Thr11) was found to be less critical for binding (13-fold reduction) and agonist activity (2-fold reduction).[13] Compounds **2**−**6** displayed poor competitive binding with GLP-1 but competed effectively with a labeled analogue of **1**. While lactam **3** was less potent than **1b**, the efficacy obtained was better than

Table 1. Affinity and Agonist Potency, on Human GLP-1R Transfected in CHO cells, of Derivatives of 1b Incorporating a Side Chain to Side Chain Cyclization Restraint between Positions 2 → 5 or 5 → 9

	linker[a] in **1b** analogues	affinity,[b,c] K_i, nM	*n*	cAMP,[c,d] EC_{50}, nM	*n*
1a		0.66 (0.17)	6	0.19 (0.019)	31
1b		0.57 (0.86)	8	0.12 (0.024)	13
2	Lys5-Asp9	59 (24)	3	68 (24)	5
3	Lys5-Glu9	17 (5.5)	8	10 (2.3)	6
4	Lys5-hGlu9	300 (60)	3	95 (25)	5
5	Asp5-Lys9	1200 (120)	3	320 (130)	4
6	Glu5-Lys9	320 (70)	8	430 (180)	5
7	Cys2-Cys5	>3100	6	670 (140)	10
8	cys2-Cys5	2400 (310)	3	600 (54)	4
9	Cys2-hCys5	980 (430)	5	190 (34)	3
10	cys2-hCys5	550 (210)	4	81 (27)	5
11	hCys2-Cys5	>8000	7	730 (200)	5
12	hcys2-Cys5	4800 (640)	3	110 (39)	4
13	hCys2-hCys5	130 (120)	8	1.8 (0.79)	4
14	hcys2-hCys5	41 (13)	3	0.73 (0.18)	7
15	hCys2-hcys5	3000 (600)	3	390 (90)	3
16	hcys2-hcys5	1700 (280)	3	200 (27)	3

[a]Lys, lysine; Asp, aspartate; Glu, glutamate; hGlu, homoglutamate; Cys, cysteine; cys, D-cysteine; hCys, homocysteine; hcys, homo-D-cysteine. Number = sequence position in **1b**. [b]Competitive binding vs **18** (Supporting Information). [c]Geometric mean with standard error in parentheses. [d]cAMP was measured in CHO cells stably transfected with human GLP-1R (Supporting Information; all compounds were full agonists relative to GLP-1 (85−107%). For compounds **2**−**16**, X_6 = αMe-2F-Phe, X_{10} = Bip, X_{11} = hhPhe. Figure S3 shows representative cAMP response curves for **1a**, **3**, and **14**.

DOI: 10.1021/acs.jmedchem.5b00166
J. Med. Chem. XXXX, XXX, XXX−XXX

expected from the Ala mutations in GLP-1. In general, the trend in affinity for this series of 11-mer ligands correlated with cAMP activity (Table 1). However, the K_i/EC_{50} ratio (Figure S1 in Supporting Information) was lower for lactams **2**, **3**, and **6** (0.75−1.6) than for **1a** and **1b** (ratio 3.5−4.7). This suggests that agonism of the lactams is more affinity driven than for the unconstrained peptides, perhaps because of the loss of Glu9. The most potent cyclic compound **3** was analyzed for structure by CD and 2D NMR spectroscopy.

A second series of compounds (**7**−**16**, Table 1) incorporated a cyclization constraint between residues 2 and 5. NMR derived structures (Figure 1B) and computer modeling studies (Figure S2, Supporting Information) indicated that Thr5 and Aib2 were close together and part of a β-turn structural motif. The distance between the α-carbons of Aib and Thr5 suggested that a linker of 4−6 heavy atoms in length might imprint a matching β-turn. Alanine mutagenesis on GLP-1 has shown that residues 2 and 5 may be altered without substantial effects on binding or cAMP function, although substituting Ala2 with Ser reduced binding by 9-fold without greatly affecting cAMP.[12] The orientation of Aib in Figures 1B and S2 showed that both stereoisomers were tolerated but with a preference for the natural configuration at Thr5. Compounds with a cysteine−cysteine or a cysteine−homocysteine linker (**7**−**12**) were found to bind hGLP-1R with low affinity (IC_{50} > 550 nM) and exhibited only moderate to weak cAMP activity (EC_{50} of 80−700 nM). Linking homocysteines at residues 2 and 5, with either LL or DL stereochemistry (**13** or **14**), improved binding affinity and cAMP activity, but LD or DD stereochemistry (**15** or **16**) reduced cAMP activity (EC_{50} > 200 nM) and binding affinity (IC_{50} > 1000 nM), consistent with the predicted geometry preference. The K_i/EC_{50} ratio (Figure S1) was higher for disulfides **12**−**14** (43−74) than for unconstrained peptides **1a**,**b** (ratio 3.5−4.7). This suggests that agonism of the disulfides is more efficacy driven than for the unconstrained 11mers, perhaps because of stabilization of a bound N-terminal turn conformation. Compound **14** was selected for solution structure analysis by NMR and CD spectra.

Circular dichroism spectra were compared to assess relative helicity in **1a**, **2**, **3**, and **14** in water vs an aqueous lipid environment (Figure 3). Compound **1a** was unstructured in

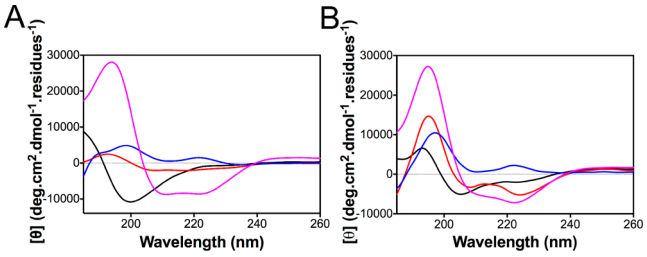

Figure 3. CD spectra of **1a** (black), **2** (pink), **3** (red), **14** (blue) at 50 μM (298 K) in (A) 10 mM aqueous phosphate (pH 7.2) and (B) aqueous 10 mM SDS.

water (Figure 3A, black) but became slightly helical in aqueous 10 mM SDS (Figure 3B, black) where the line shape (ratio θ_{222}:θ_{208} < 0.5) is consistent with some turn character, as suggested for the N-terminus by NMR data (Figures 1A, 2A). In contrast, the CD spectrum for **2** in water (Figure 3A, pink) showed a molar ellipticity maximum (197 nm) and two minima (222, 208 nm; ratio 1:1), indicative of a highly α-helical structure. The CD spectra for **3** and **14** had very weak intensity bands in water (Figure 3A, red and blue, respectively), consistent with more turn-like structure. However, **3** was more helix-like in aqueous SDS (Figure 3B, red), while **14** changed little with positive molar ellipticity attributed to D-homocysteine at position 2 (Figure 3B, blue). Given high affinities and agonist potencies for **3** and **14**, we decided to use NMR spectroscopy to more closely examine their solution structures.

The NMR-derived solution structure for **3** in 25 mM SDS-d_{25} in water is shown below (Figure 4). As expected from above,

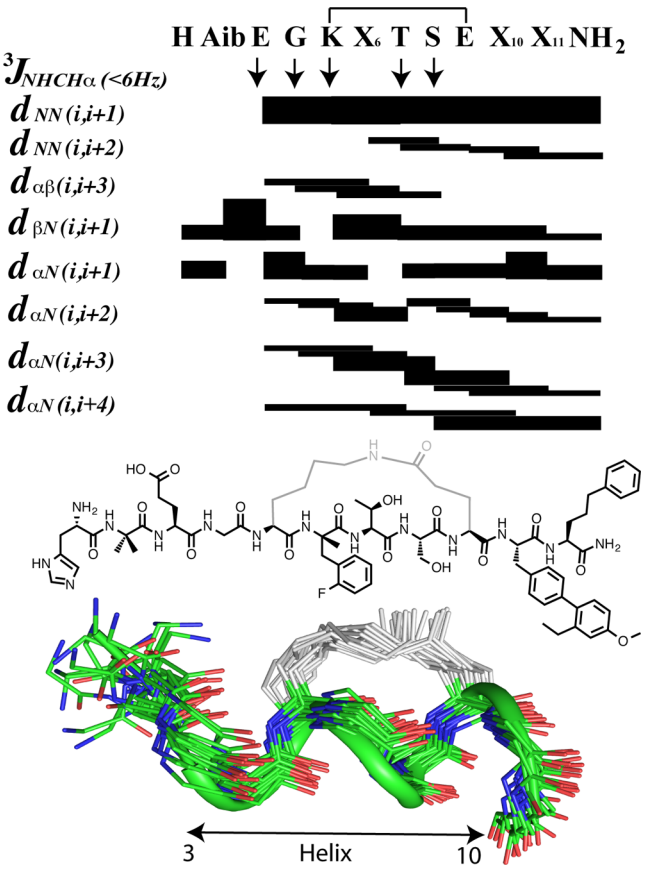

Figure 4. NMR structure summary for **3** (1 mM) in 25 mM SDS-d_{25} in water at 298 K. Top: ^{1}H NMR data summary showing sequential and medium range NOEs, with bar thickness proportional to strong (upper distance constraint 2.7 Å), medium (3.5 Å), weak (5.0 Å), and very weak (6.0 Å): $^3J_{NHCHa} \leq 6$ Hz (↓) NOE intensities. Bottom: Backbone superimposition from residues 1−11 of 20 lowest energy refined structures (peptide side chains omitted for clarity; carbon, green; nitrogen, blue; hydrogen, white; oxygen, red; lactam bridge K5-E9, gray). X6 = αMe-2F-Phe, X10 = biphenyl, X11= hhPhe.

there was evidence of distinct helical structure between residues 3 and 10, with a more flexible N-terminus. The presence of $d_{\alpha N(i,i+3)}$ and $d_{\alpha N(i,i+4)}$ along with $d_{NN(i,i+1)}$ and $d_{\alpha\beta(i,i+3)}$ suggested the structure is α-helical for the peptide in this solvent mixture.

An NMR-derived solution structure was also calculated for **14** in H_2O/DMSO-d_6 (1:3) (Figure 5), which is the most potent agonist in the second series. At the N-terminus, cross-linking residues 2 and 5 via coupling D-homocysteine to L-homocysteine side chains restrained the cyclic tetrapeptide segment (hc-E-G-hC) into a type II β-turn conformation, as revealed by the $d_{\alpha N(i,i+2)}$ NOEs observed in this region. The average $C_\alpha\cdots C_\alpha$ distance between residues 2 and 5 in these NMR structures is 5.5 Å. This is very similar to the average corresponding distances (5.6 Å) found for the unconstrained peptide **1b** in H_2O/DMSO-d_6

DOI: 10.1021/acs.jmedchem.5b00166
J. Med. Chem. XXXX, XXX, XXX−XXX

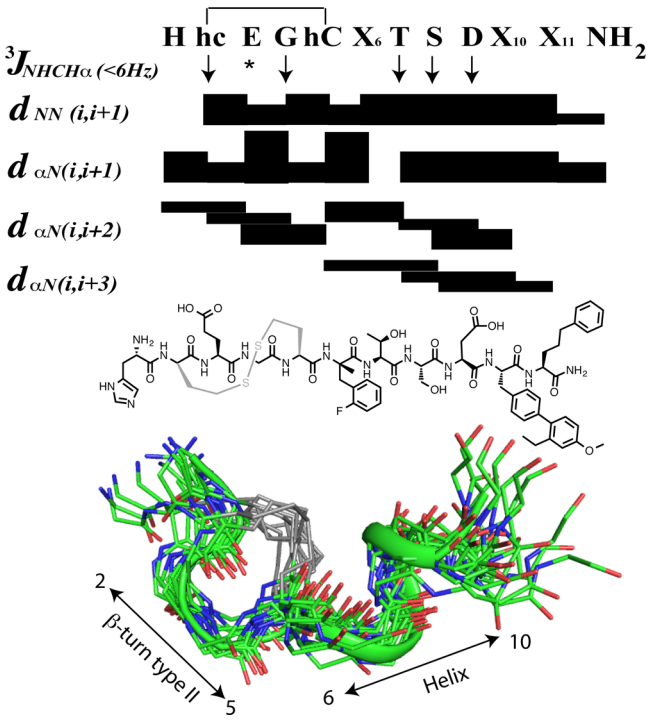

Figure 5. NMR structure summary for **14** (1 mM) in H_2O/DMSO-d_6 (1:3) at 298 K. Top: ^{1}H NMR summary showing sequential and medium range NOEs, with bar thickness proportional to strong (upper distance constraint 2.7 Å), medium (3.5 Å), weak (5.0 Å), and very weak (6.0 Å) NOE intensities: $^3J_{NHCHa} \leq 6$ Hz (↓) and broad singlet (∗). Bottom: Backbone superimposition from residues 5−10 of 10 lowest energy refined structures (peptide side chains omitted for clarity; carbon, green; nitrogen, blue; hydrogen, white; oxygen, red; disulfide bridge hc2-hC5, gray). X6 = αMe-2F-Phe, X10 = biphenyl, X11 = hhPhe.

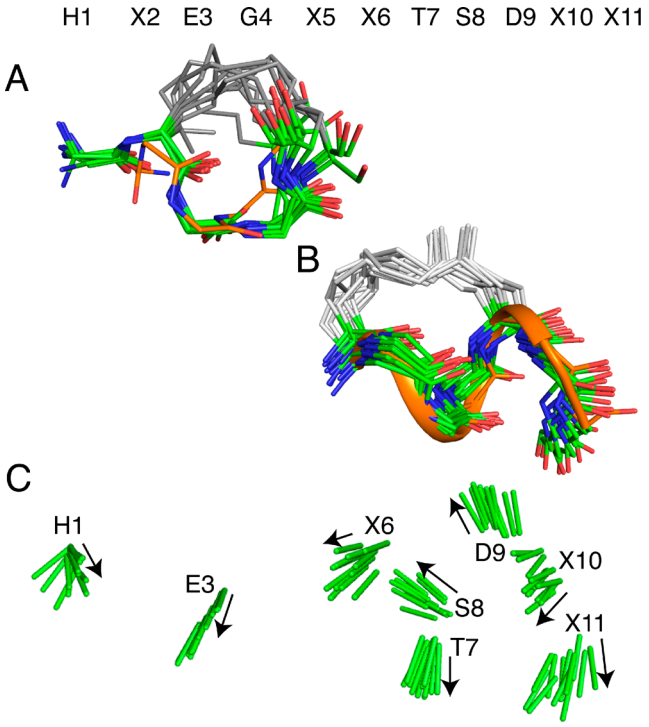

Figure 6. Combination of N-terminal β-turn (from **14**) and C-terminal α-helix (from **3**) compared with **1a** (orange). (A) Superimposed backbone residues 1−5 from NMR-derived structures of peptides **1a** and **14** superimposed in H_2O/DMSO-d_6 (1:3). Average rmsd = 1.92 Å. (B) Superimposed backbone residues 5−11 from NMR-derived structures of peptides **1a** and **3** in 25 mM SDS-d_{25} in water. Average rmsd = 0.40 Å. (C) Cα−Cβ vector topologies (arrows) for side chains of residues important for agonist activity. Peptide side chains are omitted for clarity; carbon, green; nitrogen, blue; hydrogen, white; oxygen, red; disulfide bridge in (A) and lactam bridge in (B), gray. X2 = hcys and X5 = hCys (in **14**). X5 = Lys and X9 = Glu (in **3**). X6 = αMe-2F-Phe. X10 = biphenyl. X11 = hhPhe. Vector coordinates in C along with all four structures (Figures 1, 4, 5) were lodged in a publicly accessible structural database.[14]

(1:3). At the C-terminus, there were small $^3J_{NHH\alpha}$ amide coupling constants, medium intensity $d_{NN(i,i+1)}$ and $d_{\alpha N(i,i+1)}$ NOEs, and stronger $d_{\alpha N(i,i+2)}$ intensities compared to $d_{\alpha N(i,i+3)}$ with unobservable $d_{\alpha N(i,i+4)}$ NOEs for residues 6−10. These data support an elongated helical structure rather than a more compact α-helix for the C-terminus of **14**. The average $C_\alpha \cdots C_\alpha$ distance between residues 6 and 10 was 7.0 Å instead of 6.1 Å in an α-helix and 8.3 Å for a 3_{10}-helix.

The two structural motifs identified in Figure 1, from the NMR structures determined for the "linear" peptide **1a** in different solvent mixtures, were superimposed (Figure 6) upon the corresponding cyclization-constrained sections of **3** and **14**. The results show that constraining the peptide through an optimized cyclization linker between residues 2 and 5 has produced a β-turn backbone segment in **14** that matches the turn structure observed for the acyclic peptide **1b** in aqueous DMSO solvent (Figure 6A). Further, the α-helix structure observed by NMR spectroscopy for **1b** in aqueous SDS is mimicked by the helix-constrained analogue **3** (Figure 6B).

By combining these two important structural features (type II β-turn and α-helix) derived from the constrained peptide analogues **14** and **3**, we created a combined topology map of Cα−Cβ bond vectors of the side chains of the amino acid residues that were most influential in determining agonist activity (Figure 6C). This map could serve as a guide for further development of peptidomimetics with β-turn and α-helix mainchain motifs and as a pharmacophore map of side chain vectors for future development of small molecule agonists for GLP-1R.

CONCLUSIONS

Solution structures were determined for the potent GLP-1R agonist **1a** in aqueous SDS versus aqueous DMSO solvent mixtures using NMR spectroscopy. They revealed two dominant structural motifs; a helical structure between residues 5 and 9 and a turn structure between residues 2 and 5. Constraining residues 5−9, using a series of lactam bridges designed to alter the nature and flexibility of the helix, reduced agonist potency and binding affinity. The most potent lactam-constrained compound **3** did not contain the most α-helical structure, but it was only slightly elongated. CD spectra supported this finding, while the NMR structure revealed that the dominant structure was mainly α-helical. The other dominant structural feature in **1a** from NMR studies was mimicked in **13** and **14** with potent cAMP activity and high receptor-binding affinity. The NMR structure of **14** revealed a type II β-turn between amino acids 2 and 5, with some elongated α-helical character retained between positions 6 and 10. These data provide important lessons for developing improved GLP-1 agonists. The helical structure, stabilized with lactams over residues 5−9, diminished efficacy more than affinity. By contrast, stabilization of a β-turn, using a disulfide

DOI: 10.1021/acs.jmedchem.5b00166
J. Med. Chem. XXXX, XXX, XXX−XXX

cross-link over residues 2−5, diminished affinity more than efficacy. These differential effects of the structural constraints on potency vs affinity of GLP-1 agonists (Figure S1) has helped to identify important structural requirements and limitations for activity of peptidomimetic and small molecule agonists of the type 2 diabetes target GLP-1R.

EXPERIMENTAL SECTION

Chemicals. See Supporting Information.

Peptide Synthesis. Peptides were synthesized by standard Fmoc chemistry methods described elsewhere.[12] Lactam bridges where formed as described previously.[12] For disulfide bridge formation, the crude linear peptide (just cleaved from resin) was dissolved in water. To the resulting aqueous solution, iodine in methanol (20 mg/mL) was added until a brown solution was afforded. Full synthetic details are provided in the Supporting Information.

Purification of Peptides. Crude peptides (pellets) were dissolved in a minimal amount of water and purified using a Waters 4000 system connected to a Waters Delta-PakTMC18, 15 μm, 100 Å reversed-phase HPLC column (25 mm × 200 mm), eluting with a solvent gradient of A and B where solvent A was 0.1% TFA in water and solvent B was 0.1% TFA in acetonitrile/water (4:1)]. The specific gradient conditions are described for final peptides. (Supporting Information) Purified peptides were analyzed to confirm >95% purity using an HP1090 system with a 4.6 mm × 150 mm SepaxGP- C18 (2), 5 μm, 120 Å column or a 4.6 × 150 mm Phenomenex C18 (2), 5 μm 100 Å column, eluting with a solvent gradient of A and C, where solvent A was 0.1% TFA in water and solvent C was 0.09% TFA in acetonitrile/water (4:1), over 20 min at a flow rate of 1.0 mL/min. The specific retention times, UV purities (220 nm), and solvent gradients are described for final peptides in the Supporting Information.

Radioligand Binding Assay. The ability of test compounds to displace a ^{125}I-labeled 11 amino acid GLP-1R agonist (**18**) was performed. Compound affinity was expressed as a K_i value, defined as the concentration of compound required to decrease **18** binding by 50% for a specific membrane batch at a given concentration of radioligand. The nonradiolabeled analogue of **18** had K_i = 6.0 (2.7) nM for binding affinity and EC_{50}= 0.045 (0.013) nM for cAMP. Full experimental details are provided in the Supporting Information.

CHO cAMP Accumulation Assay. CHO cells stably transfected with hGLP-1R were incubated (37 °C, 95% O_2, 5% CO_2) in flasks containing DMEM/F12 (1:1) media supplemented with 1% GlutaMAX (Gibco), 1% PenStrep, and 1% Geneticin (Gibco). Following LANCE Ultra cAMP assay (PerkinElmer) manufacturer's instructions, cells were washed (PBS), lifted (cell dissociation solution), centrifuged (1500 rpm, 5 min), resuspended in cAMP assay buffer (HBSS, 5.56 mM glucose, 0.1% BSA (final), 0.5 mM IBMX (final), 5 mM HEPES (final)) and seeded (1000 cells/well) in a ProxiPlate-384 Plus plate (PerkinElmer). Cells were treated with compounds (10 μM to 100 fM) diluted in assay buffer at room temp for 30 min. Cell lysis buffer plus Tracer (1:50) or Ulight (1:150) (supplied in cAMP assay kit) were added to each well and incubated covered at room temp for 2 h before the plate was read on a PHERAstar FS (BMG Labtech). For analysis, compound raw signal was normalized to a percentage of GLP-1 maximum raw signal.

CD measurements were performed using a Jasco model J-710 spectropolarimeter as previously described. Full experimental details are described in the Supporting Information.

NMR Spectroscopy and Structure Calculations. Full experimental details are provided in the Supporting Information.

ASSOCIATED CONTENT

Supporting Information

Synthetic methods, compound characterization, cAMP and binding affinity experiments, CD methods, NMR calculations, and NMR spectra. This material is available free of charge via the Internet at http://pubs.acs.org.

AUTHOR INFORMATION

Corresponding Authors

*D.A.G.: e-mail, david.a.griffith@pfizer.com; phone, 860-441-6215.

*D.P.F.: e-mail: d.fairlie@imb.uq.edu.au; phone, 61 7 3346 2989.

Notes

The authors declare no competing financial interest.

ACKNOWLEDGMENTS

We thank the Australian National Health and Medical Research Council for a Senior Principal Research Fellowship to D.P.F. (Grant 1027369) and the Australian Research Council for Grants LP110200213, DP130100629 and for a Centre of Excellence in Advanced Molecular Imaging Grant CE140100011. We also thank the Pfizer Emerging Science fund for support.

ABBREVIATIONS USED

2D NMR, two dimensional nuclear magnetic resonance; CHO, Chinese hamster ovary; GLP-1, glucagon-like peptide-1; GLP-1R, GLP-1 receptor; hC, homocysteine; hhPhe, homohomophenylanaline; hGlu, homoglutamic acid; VT, variable temperature; DMEM, Dulbecco's modified Eagle medium; HBSS, Hanks' balanced salt solution; IBMX, 3-isobutyl-1-methylxanthine; HEPES, 4-(2-hydroxyethyl)-1-piperazineethanesulfonic acid

REFERENCES

(1) (a) Scully, T. Diabetes in numbers. *Nature* **2012**, *485*, S2−S3. (b) Shi, Y.; Hu, F. B. The global implications of diabetes and cancer. *Lancet* **2014**, *383*, 1947−1948. (c) Smyth, S.; Heron, A. Diabetes and obesity: the twin epidemics. *Nat. Med.* **2006**, *12*, 75−80.

(2) (a) Drucker, D. J. The biology of incretin hormones. *Cell Metab.* **2006**, *3*, 153−165. (b) Drucker, D. J.; Nauck, M. A. The incretin system: glucagon-like peptide-1 receptor agonists and dipeptidyl peptidase-4 inhibitors in type 2 diabetes. *Lancet* **2006**, *368*, 1696−1705. (c) Holst, J. J.; Vilsboll, T.; Deacon, C. F. The incretin system and its role in type 2 diabetes mellitus. *Mol. Cell. Endocrinol.* **2009**, *297*, 127−136.

(3) Holst, J. J. The physiology of glucagon-like peptide 1. *Physiol. Rev.* **2007**, *87* (4), 1409−1439.

(4) (a) Bode, B. Liraglutide: a review of the first once-daily GLP-1 receptor agonist. *Am. J. Managed Care* **2011**, *17*, S59−S70. (b) Jespersen, M. J.; Knop, F. K.; Christensen, M. GLP-1 agonists for type 2 diabetes: pharnnacokinetic and toxicological considerations. *Expert Opin. Drug Metab. Toxicol.* **2013**, *9*, 17−29.

(5) (a) Neumiller, J. J.; Wood, L.; Campbell, R. K. Dipeptidyl peptidase-4 inhibitors for the treatment of type 2 diabetes mellitus. *Pharmacotherapy* **2010**, *30*, 463−484. (b) Duez, H.; Cariou, B.; Staels, B. DPP-4 inhibitors in the treatment of type 2 diabetes. *Biochem. Pharmacol.* **2012**, *83*, 823−832.

(6) (a) Edmonds, D. J.; Price, D. A. Oral GLP-1 modulators for the treatment of diabetes. *Annu. Rep. Med. Chem.* **2013**, *48*, 119−130. (b) Manandhar, B.; Ahn, J. M. Glucagon-like peptide-1 (GLP-1) analogs: Recent advances, new possibilities, and therapeutic implications. *J. Med. Chem.* **2015**, *58*, 1020−1037.

(7) (a) Runge, S.; Thogersen, H.; Madsen, K.; Lau, J.; Rudolph, R. Crystal structure of the ligand-bound glucagon-like peptide-1 receptor extracellular domain. *J. Biol. Chem.* **2008**, *283*, 11340−11347. (b) Runge, S.; Schimmer, S.; Oschmann, J.; Schiodt, C. B.; Knudsen, S. M.; Jeppesen, C. B.; Madsen, K.; Lau, J.; Thogersen, H.; Rudolph, R. Differential structural properties of GLP-1 and exendin-4 determine their relative affinity for the GLP-1 receptor N-terminal extracellular domain. *Biochemistry* **2007**, *46*, 5830−5840.

(8) Siu, F. Y.; He, M.; de Graaf, C.; Han, G. W.; Yang, D.; Zhang, Z.; Zhou, C.; Xu, Q.; Wacker, D.; Joseph, J. S.; Liu, W.; Lau, J.; Cherezov, V.;

DOI: 10.1021/acs.jmedchem.5b00166
J. Med. Chem. XXXX, XXX, XXX−XXX

Katritch, V.; Wang, M.-W.; Stevens, R. C. Structure of the human glucagon class B G-protein-coupled receptor. *Nature* **2013**, *499*, 444.

(9) (a) MontroseRafizadeh, C.; Yang, H.; Rodgers, B. D.; Beday, A.; Pritchette, L. A.; Eng, J. High potency antagonists of the pancreatic glucagon-like peptide-1 receptor. *J. Biol. Chem.* **1997**, *272*, 21201−21206. (b) Adelhorst, K.; Hedegaard, B. B.; Knudsen, L. B.; Kirk, O. Structure-activity studies of glucagon-like peptide-1. *J. Biol. Chem.* **1994**, *269*, 6275−6278. (c) Gefel, D.; Hendrick, G. K.; Mojsov, S.; Habener, J.; Weir, G. C. Glucagon-like peptide-1 analogs: effects on insulin-secretion and adenosine-3′,5′-monophosphate formation. *Endocrinology* **1990**, *126*, 2164−2168. (d) Suzuki, S.; Kawai, K.; Ohashi, S.; Mukai, H.; Yamashita, K. Comparison of the effects of various c-terminal and n-terminal fragment peptides of glucagon-like peptide-1 on insulin and glucagon-release from the isolated perfused rat pancreas. *Endocrinology* **1989**, *125*, 3109−3114.

(10) Mapelli, C.; Natarajan, S. I.; Meyer, J.-P.; Bastos, M. M.; Bernatowicz, M. S.; Lee, V. G.; Pluscec, J.; Riexinger, D. J.; Sieber-McMaster, E. S.; Constantine, K. L.; Smith-Monroy, C. A.; Golla, R.; Ma, Z.; Longhi, D. A.; Shi, D.; Xin, L.; Taylor, J. R.; Koplowitz, B.; Chi, C. L.; Khanna, A.; Robinson, G. W.; Seethala, R.; Anatal-Zimanyi, I. A.; Stoffel, R. H.; Han, S.; Whaley, J. M.; Huang, C. S.; Krupinski, J.; Ewing, W. R. Eleven amino acid glucagon-like peptide-1 receptor agonists with antidiabetic activity. *J. Med. Chem.* **2009**, *52*, 7788−7799.

(11) Haque, T. S.; Lee, V. G.; Riexinger, D.; Lei, M.; Malmstrom, S.; Xin, L.; Han, S.; Mapelli, C.; Cooper, C. B.; Zhang, G.; Ewing, W. R.; Krupinski, J. Identification of potent 11mer glucagon-like peptide-1 receptor agonist peptides with novel C-terminal amino acids: homohomophenylalanine analogs. *Peptides* **2010**, *31*, 950−955.

(12) (a) Shepherd, N. E.; Hoang, H. N.; Abbenante, G.; Fairlie, D. P. Single turn peptide alpha helices with exceptional stability in water. *J. Am. Chem. Soc.* **2005**, *127* (9), 2974−2983. (b) Harrison, R. S.; Shepherd, N. E.; Hoang, H. N.; Ruiz-Gomez, G.; Hill, T. A.; Driver, R. W.; Desai, V. S.; Young, P. R.; Abbenante, G.; Fairlie, D. P. Downsizing human, bacterial, and viral proteins to short water-stable alpha helices that maintain biological potency. *Proc. Natl. Acad. Sci. U.S.A.* **2010**, *107*, 11686−11691.

(13) Murage, E. N.; Schroeder, J. C.; Beinborn, M.; Ahn, J. M. Search for alpha-helical propensity in the receptor-bound conformation of glucagon-like peptide-1. *Bioorg. Med. Chem.* **2008**, *16*, 10106−10112.

(14) Biological Magnetic Resonance Bank (PDB numbers for **1a** in 25 mM SDS-d_{25} in water (2n08); **1a** in H_2O/DMSO-d_6 (1:3) (2n09); **3** (2n0n) and **14** (2n0i)).

DOI: 10.1021/acs.jmedchem.5b00166
J. Med. Chem. XXXX, XXX, XXX−XXX